

Functional features of crossmodal mismatch responses

Chen Zhao · Elia Valentini · Li Hu

Received: 20 August 2014 / Accepted: 2 November 2014 / Published online: 15 November 2014
© Springer-Verlag Berlin Heidelberg 2014

Abstract Research on brain mechanisms of deviance detection and sensory memory trace formation, best indexed by the mismatch negativity, mainly relied on the investigation of responses elicited by auditory stimuli. However, comparable less research reported the mismatch negativity elicited by somatosensory stimuli. More importantly, little is known on the functional features of mismatch deviant and standard responses across different sensory modalities. To directly compare different sensory modalities, we adopted a crossmodal roving paradigm and collected event-related potentials elicited by auditory, non-nociceptive somatosensory, and nociceptive trains of stimuli, during Active and Passive attentional conditions. We applied a topographical segmentation

analysis to cluster successive scalp topographies with quasi-stable landscape of significant differences to extract crossmodal mismatch responses. We obtained three main findings. First, across different sensory modalities and attentional conditions, the formation of a standard sensory trace became robust mainly after the second stimulus repetition. Second, the neural representation of a modality deviant stimulus was influenced by the preceding sensory modality. Third, the mismatch negativity significantly covaried between Active and Passive attentional conditions within the same sensory modality, but not between different sensory modalities. These findings provide robust evidence that, while different modalities share a similar process of standard trace formation, the process of deviance detection is largely modality dependent.

Chen Zhao and Elia Valentini have contributed equally to this work.

Electronic supplementary material The online version of this article (doi:[10.1007/s00221-014-4141-4](https://doi.org/10.1007/s00221-014-4141-4)) contains supplementary material, which is available to authorized users.

C. Zhao · L. Hu (✉)

Key Laboratory of Cognition and Personality (Ministry of Education) and Faculty of Psychology, Southwest University, Chongqing, China
e-mail: hulitju@gmail.com

C. Zhao

Institute of Brain, Behaviour and Mental Health, Faculty of Medical and Human Sciences, The University of Manchester, Manchester, United Kingdom

E. Valentini

Psychology Department, Sapienza University of Rome, Rome, Italy

E. Valentini

Scientific Institute for Research, Hospitalization and Health Care, Santa Lucia Foundation, Rome, Italy

Keywords Event-related potentials (ERPs) · Roving paradigm · Deviance detection · Standard formation · Crossmodal mismatch response

Introduction

A flourishing domain of investigation in neuroscience during the last 30 years revolves around the notion that the brain is equipped with mechanisms able to generate mnemonic models of sensory invariance in the environment while scanning it to detect changes, which may either confirm or disconfirm the brain's statistical models. The detection of deviance requires the prior detection and consolidation of regularity extracted from the previous inputs. The new input is then compared to this regularity representation, and a mismatch process is elicited in case of a model violation (Näätänen et al. 2007; Pakarinen et al. 2010). The most replicated experimental paradigm for testing these very mechanisms relied on the application of electrophysiological

methods such as electroencephalography (EEG) or magnetoencephalography (MEG) to measure event-related ‘mismatch negativity’ (MMN) in response to violations of expectancy or learned regularities. This MMN is normally obtained in the context of odd-ball paradigms (Näätänen et al. 1992). Otherwise, a stimulation protocol with a continuously changing (‘roving’) sensory input is implemented (Baldeweg et al. 2004).

Most of MMN findings originated from studies in the auditory domain, showing that auditory MMN peaks at about 100–250 ms and is maximal at fronto-temporal regions (Sams et al. 1985). However, far less research has been carried out to investigate mismatch-related responses in other sensory modalities, especially in the somatosensory modality (e.g., Kekoni et al. 1997). This discrepancy between sensory modalities may be related to the inherent low signal-to-noise ratio of MMN (Cacace and McFarland 2003; Butler et al. 2012). Even when elicited by auditory stimuli, the MMN is normally no more than 5 μ V, on average across several individuals (Näätänen et al. 2007). This fact hampers the detection of MMN activity in non-nociceptive somatosensory and nociceptive systems, where the signal-to-noise ratio is even lower and a clear MMN peak may be absent at single-subject level (Näätänen et al. 2011; Butler et al. 2012). Therefore, direct comparison of functional features of mismatch responses across different sensory modalities is currently lacking, thus hindering the understanding of similarities and differences in the basic mechanisms of deviance detection and regularity representation across different sensory systems.

We recently investigated the potential of detecting and measuring a MMN elicited by nociceptive stimulation as compared to non-nociceptive somatosensory stimulation (Hu et al. 2013). In both modalities, deviance detection was determined by introducing a change in the spatial location of the stimuli (i.e., unimodal mismatch response). However, previous evidences showed that the introduction of a change in the stimulus modality (i.e., crossmodal mismatch response), rather than in the spatial location of a stimulus, was more effective in enhancing the magnitude of the deviant response (Valentini et al. 2011; Torta et al. 2012). Bearing on these findings, here we implemented a crossmodal roving paradigm that aimed to (1) increase the signal-to-noise ratio of deviant responses in different sensory modalities and (2) directly compare mismatch responses across different sensory modalities. To improve the separation of these responses, we combined the topographical segmentation analysis (Lehmann et al. 1987) with the cluster-based statistical test (Maris and Oostenveld 2007). This approach allowed us to test whether the neural activity associated to deviance detection in the auditory, non-nociceptive somatosensory, and nociceptive modalities can be considered as modality dependent or modality independent.

Materials and methods

Participants

EEG data were collected from 30 healthy right-handed volunteers (15 males and 15 females), aged 22 ± 1.7 (mean \pm SD, range 18–26 years). All participants gave their written informed consent and were paid for their participation. The local ethics committee of Southwest University (Chongqing, China) approved the procedures, which were in accordance with the standards of the declaration of Helsinki.

Stimulation

Auditory stimuli were brief 800 Hz tones (50 ms duration; 5 ms rise and fall times) presented at ~85 dB SPL and delivered through a loudspeaker. Non-nociceptive somatosensory stimuli (i.e., transcutaneous electrical stimuli, TES) consisted of three rapidly succeeding constant-current square-wave pulses (0.5 ms duration) delivered through a pair of ring electrodes (2 cm distance between electrodes) applied to the index finger, between the metacarpophalangeal and the interphalangeal joint. The inter-pulse interval was 12 ms. The stimulus intensity was twice the individual perceptual threshold, an intensity classically used to activate the A β fibers in humans (Garcia-Larrea et al. 1995; Hu et al. 2011). These stimuli elicited a vibratory sensation and were never reported as painful. Nociceptive stimuli (i.e., intra-epidermal electrical stimuli, IES) consisted of three rapidly succeeding constant-current square-wave pulses (0.5 ms duration) delivered through three stainless steel concentric bipolar needle electrodes (located according to an equilateral triangle shape) to the median section of the hand. Each of the electrode consisted of a needle cathode (length: 0.1 mm, Ø: 0.2 mm) surrounded by a cylindrical anode (Ø: 1.4 mm) (Inui et al. 2002, 2006). The inter-pulse interval was 12 ms. The stimulus intensity was twice the individual perceptual threshold, an intensity that has been proved to preferentially activate the A δ nociceptive fibers without to simultaneously activate the A β fibers (Mouraux et al. 2010). These stimuli elicited a painful pinprick sensation in all the participants. All sensory stimuli were delivered at or near the hand (left hand for 22 participants and right hand for eight participants). The position of the auditory stimulator was adjusted until the participants reported similar spatial location for three sensory modalities (Liang et al. 2010).

Experimental design

Participants seated on a comfortable chair in a silent, temperature-controlled room. Prior to data collection,

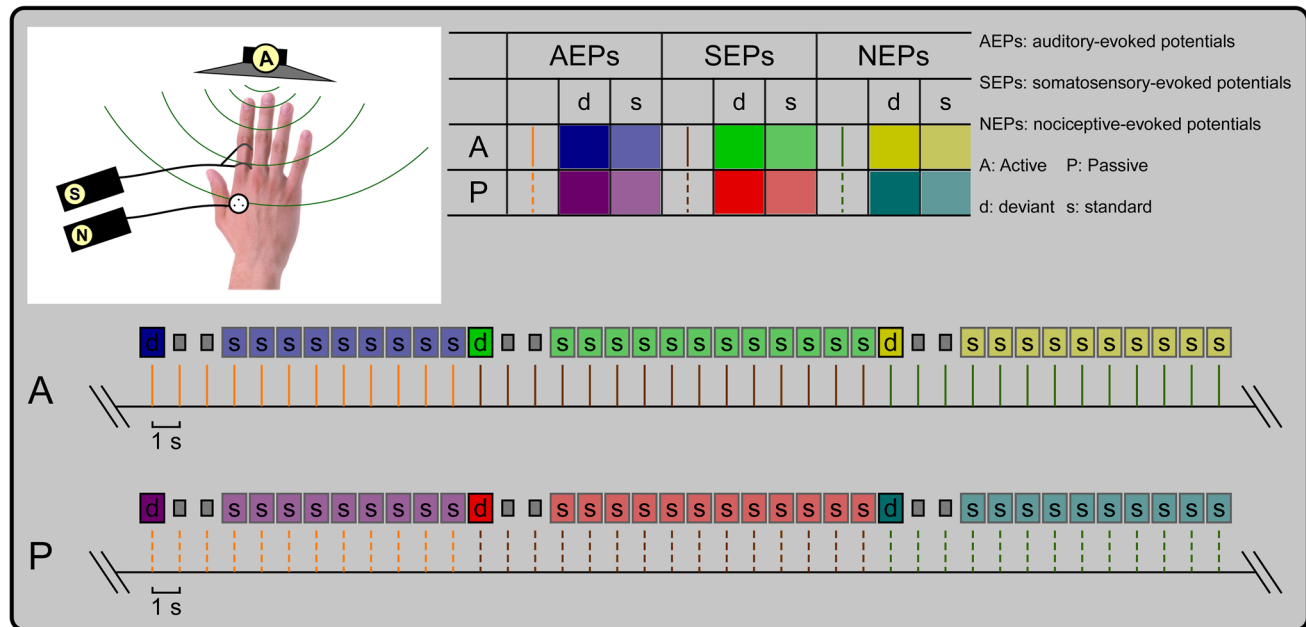


Fig. 1 Experimental design. Auditory evoked potentials (AEPs), non-nociceptive somatosensory evoked potentials (SEPs), and nociceptive evoked potentials (NEPs) were recorded from stimuli delivered through a loudspeaker located near the stimulated hand, a pair of ring electrodes applied to the index finger of the dominant hand, and a set of three bipolar needle electrodes applied to the median section of the hand (A, S, and N, top left). AEPs, SEPs, and NEPs were recorded while participants were required to focus their attention either on the incoming deviant and standard stimuli (A: Active condition) or on watching a silent video with subtitles (P: Passive condition)

tion; *top central*). In the roving paradigm, the first stimulus in each train was a deviant (d) that became a standard (s) through repetition. The sensory events representing the transition (the second and third stimuli in a train) from the deviant to the purported standard events are depicted with gray squares. Trains of auditory, non-nociceptive somatosensory, and nociceptive stimuli were pseudo-randomly presented in the same block while making sure that two successive trains were always belonging to different modalities. The inter-train interval was 1,000 ms, and in each train, 11–15 repeated identical stimuli were delivered with an inter-stimulus interval of 1,000 ms (*bottom*)

participants were familiarized with all sensory stimuli and they had no difficulty in distinguishing each stimulus modality. Auditory, non-nociceptive somatosensory, and nociceptive evoked potentials (AEPs, SEPs, and NEPs) were elicited by trains of auditory tones, non-nociceptive TES, and nociceptive IES, respectively (Fig. 1, top left). The sensory events were administered according to a classical roving paradigm (Garrido et al. 2008). The first stimulus in each train was a deviant (d) that became a standard (s) through repetition (Fig. 1, top central). Also, the design implied that AEPs, SEPs, and NEPs were recorded either while the participants were attending to (Active condition), or were distracted from (Passive condition), the sensory stimuli (Fig. 1, top central). In Active blocks, participants were instructed to focus on the stimuli and required to report the total number of the stimuli at the end of each block. If a participant could not report the total number of stimuli or reported a wrong value, the corresponding Active block was discarded, and another block was started. In addition, at the end of each Active block, participants were required to verbally rate the average intensity of the sensation associated to sensory stimuli belonging to each modality, using a numerical rating scale ranging from 0

to 10, where 0 was ‘no sensation’ and 10 was ‘unbearable sensation.’ In Passive blocks, participants were instructed to watch a silent video with subtitles and required to answer general and specific questions about the video content in a structured interview taking place at the end of each Passive block.

The whole experiment contained 14 blocks (seven blocks per attention condition). The order of all blocks was counterbalanced across participants. Each block lasted for about 6 min and contained 26 or 24 trains of stimuli with an inter-train interval of 1,000 ms. The participant had a break of 2 min between consecutive blocks, and the whole experiment lasted for about 120 min. The total number of trains for each condition (Active or Passive) and each sensory modality (auditory, non-nociceptive somatosensory, and nociceptive) was 60 (120 trains for each modality irrespective of the attentional condition). Trains of auditory, non-nociceptive somatosensory, and nociceptive stimuli were pseudo-randomly presented in the same block (according to the rule that two successive trains were always belonging to different modalities), as well as the number of stimuli in each train was pseudo-randomly distributed across trains. There were five different train lengths (ranging from 11

to 15 stimuli), and the sensory events were separated by 1,000 ms inter-stimulus interval (Fig. 1, bottom). Note that the number of trains per train length within each modality ($n = 24$, 120/5) was the same for each participant.

EEG recording

The EEG data were recorded using a Brain Products system (band-pass: 0.01–100 Hz, sampling rate: 1,000 Hz), which was connected to a standard EEG cap with 64 scalp Ag–AgCl electrodes placed according to the international 10–20 system. The nose was used as reference channel, and all channel impedances were kept below 10 k Ω . To monitor ocular movements and eye blinks, electrooculographic signals were simultaneously recorded from two surface electrodes placed over the lower eyelid and 1 cm lateral to the outer corner of the orbit, respectively.

Data analysis

EEG data preprocessing

EEG data were processed using EEGLAB (Delorme and Makeig 2004), an open source toolbox running in the MATLAB environment. Continuous EEG data were low-pass filtered at 30 Hz. EEG epochs were extracted using a time window of 1,000 ms (200 ms prestimulus and 800 ms poststimulus) and baseline corrected using the prestimulus interval. Trials contaminated by eye blinks and movements were corrected using an independent component analysis algorithm (Delorme and Makeig 2004). In all datasets, these independent components had a large electrooculographic channel contribution and a frontal scalp distribution. After independent component analysis, epochs were rereferenced to a common average reference. EEG data, collected from all participants, were analyzed together by flipping the left and right electrodes of eight participants (Miura et al. 2003; MacDonald et al. 2004; Crucu et al. 2008), whose sensory stimuli were delivered to or near the right hand. The operation of flipping the left and right electrodes should have not biased our observation since the auditory MMN was bilaterally distributed (Sams et al. 1985; Doeller et al. 2003; Opitz et al. 2005; Näätänen et al. 2011), and the non-nociceptive somatosensory MMN and nociceptive MMN showed both contralateral and bilateral distributions (Akatsuka et al. 2007; Chen et al. 2008). For each sensory modality (auditory, non-nociceptive somatosensory, and nociceptive), attentional condition (Active and Passive), and stimulus position in the train (first, second, ..., tenth, and last), the epochs were averaged across trials in each participant. This procedure yielded 22 average waveforms in each participant and sensory modality.

Analytical approach to the extraction of mismatch negativity

A point-to-point, two-way repeated measures analysis of variance (ANOVA) was used to assess the effects of ‘repetition’ (eleven levels: first, second, ..., tenth, and last) and ‘attention’ (two levels: Active and Passive) on AEPs, SEPs, and NEPs, respectively. This procedure yielded three time courses of F values for each modality and channel representing (1) the main effect of ‘repetition,’ (2) the main effect of ‘attention,’ and (3) their interaction.

It is important to note that the obtained significance may be long lasting with variable scalp distributions (Appendix 1, ESM), and therefore, the definition of temporal interval of interests (IOIs) could be optimally achieved by utilizing not only the temporal adjacency but also the scalp distribution of F values. For this reason, single-electrode ERPs were then followed by a point-by-point linear regression analysis, with ERP amplitude as dependent variable and stimulus position in the train as predictor, per modality. If a positive or negative regression coefficient was observed, the F value representing the main effect of ‘repetition’ was, respectively, assigned to a minus or plus sign. It is important to highlight that: (1) the absolute F value would not change in magnitude as a function of the attributed regression coefficient and (2) the amplitude reduction of positive and negative potentials would be assigned to a different F sign, which ensured the distinction of repetition-modulated positive and negative brain potentials. The characterization of the effect of ‘repetition’ combined with the regression analysis was meant to assess whether the stimulus position in a train (i.e., its position in a time series of repeated events) exerted a modulation of brain responses regardless of the factor ‘attention,’ and thus allowed us to achieve one of the objectives of the present study: the identification of robust standard formation for each modality.

A topographical segmentation analysis was performed on the ‘repetition-’ modulated and signed F time courses in each sensory modality. This analysis is conceptually identical to the method of functional microstates (Michel et al. 2001) defined as a temporal parceling of successive scalp topographies with quasi-stable landscape (Lehmann and Skrandies 1980; Murray et al. 2008). Thus, the scalp topographies of ‘repetition-’ modulated and signed F values were parsed into different temporal IOIs, using a statistical method based on a modified version of the classical k -means clustering analysis (i.e., subspace pattern recognition). The optimal number of segmentations (temporal IOIs) was determined by the minimization of one of the cross-validation residual variance estimators (Pascual-Marqui et al. 1995). Indeed, the subspace pattern recognition method ensures that (1) the difference between segmentation and measurement (signed F values) is small and that

(2) the majority of the nearby measurements belongs to the same segmentation. As far as possible MMN-related brain responses were concerned, temporal IOIs, which met the following criteria, were considered in the analysis (Fig. 2): (1) resulted in clusters included in the time interval from 0 to 250 ms; (2) showed an increased global field power (GFP) as compared to the GFP within the prestimulus time interval (−200 to 0 ms); (3) lasted longer than 80 ms; and (4) displayed negative scalp topographies according to the classical polarity of the MMN.

For each MMN IOI and sensory modality, the mean ERP amplitudes of all time points (within the MMN IOI) and electrodes (showing the strongest negative modulation with stimulus repetition) were calculated at each stimulus position and attentional condition. Two-way repeated measures ANOVA was used to assess the effects of ‘repetition’ (eleven levels: first, second, ..., tenth, and last) and ‘attention’ (two levels: Active and Passive) on the mean ERP amplitudes for each sensory modality. When the interaction was significant, post hoc Tukey’s HSD test was performed. The neural representation of *standard* activity was defined based on the emergent data profile using the following criteria: (1) the activity associated to each tested stimulus position had to be significantly different from the activity evoked by the first stimulus in the train (deviant); (2) the activity associated to the tested stimulus position had to be not significantly different from the activity evoked by three other repeated stimuli (i.e., except the first stimulus) in the train. Based on the results that amplitudes changed minimally after the third train position for all modalities and both attentional conditions (see “Results” section for details), and to facilitate the achievement of a high signal-to-noise ratio of standard responses, we defined the first stimulus in each train as the deviant stimulus, and the fourth to the last stimuli in each train as the standard stimuli (i.e., standard responses were the mean of responses to the fourth to the last stimuli). To assess the influence of preceding modality on the neural representation of deviance detection and standard formation, we calculated deviant and standard responses for each preceding sensory modality, sensory modality, and attentional condition, respectively. Amplitudes of deviant and standard responses within the MMN IOI at electrodes showing the largest MMN amplitude were calculated for each preceding sensory modality, sensory modality, and attentional condition. Two-way repeated measures ANOVA was used to assess the effects of ‘preceding modality’ (two levels: non-nociceptive somatosensory and nociceptive for AEPs; auditory and nociceptive for SEPs; and auditory and non-nociceptive somatosensory for NEPs) and ‘attention’ (two levels: Active and Passive) on the estimated amplitudes for each sensory modality and each response type (deviant and

standard). When the interaction was significant, post hoc Tukey’s HSD test was performed.

The differences (deviant–standard) of amplitudes within the MMN IOI at the electrodes showing the largest MMN amplitude were calculated for each sensory modality and attentional condition. Correlation coefficients and their significance of different amplitudes were calculated using Pearson correlation analysis (1) between two attentional conditions for each sensory modality; (2) between pairs of sensory modalities in the Active condition; (3) between pairs of sensory modalities in the Passive condition. The obtained significances were adjusted using Bonferroni correction.

Results

Psychophysics

In the Active condition, the average ratings (\pm SEM) of the intensity of perception associated to auditory, non-nociceptive somatosensory, and nociceptive stimuli were $5.43 \pm .21$, $5.53 \pm .24$, and $4.53 \pm .21$, respectively.

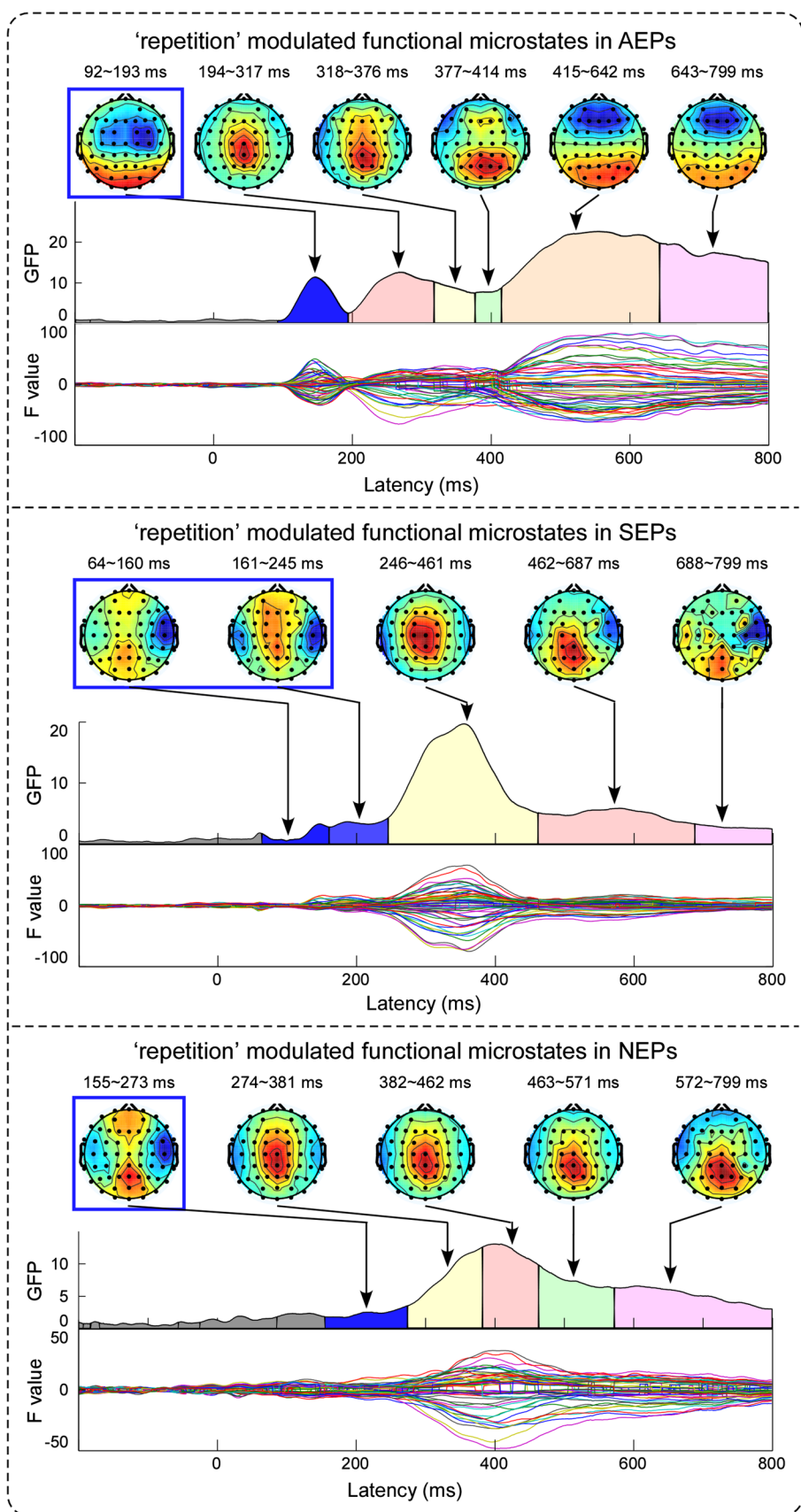
MMN temporal IOIs

Figure 2 shows time courses, GFPs, and scalp topographies of ‘repetition-’ modulated and signed F values in AEPs (top), SEPs (middle), and NEPs (bottom). The optimal number of temporal IOIs, estimated using the cross-validation criterion, was six for AEPs, and five for SEPs as well as for NEPs. A MMN IOI in AEPs at 92–193 ms was detected, which showed negativity at bilateral fronto-central region (maximal around FC1, FC2, FC3, and FC4) (Fig. 2, top). Two MMN IOIs in SEPs at 64–160 ms (first MMN IOI) and at 161–245 ms (second MMN IOI) were detected, which showed a negativity at bilateral temporal regions (maximal around FC6, C6 and C6, CP6, respectively) (Fig. 2, middle). A MMN IOI in NEPs at 155–273 ms was detected, which showed negativity at bilateral temporal regions (maximal around FC6 and C6) (Fig. 2, bottom).

Effect of ‘repetition’ and ‘attention’ of MMN IOIs

Figure 3 shows time courses of AEPs (measured at FC1, FC2, FC3, and FC4), SEPs (measured at FC6, C6 and C6, CP6, respectively), and NEPs (measured at FC6 and C6) to repeated stimuli (first, second, ..., tenth, and last) in both Active (top, upper plots) and Passive (top, lower plots) conditions. Two-way repeated measures ANOVA revealed that amplitudes of AEPs within the MMN IOI were significantly modulated by ‘repetition’ ($F_{(1,29)} = 12.73$,

Fig. 2 Topographical segmentation analysis to extract ‘repetition’- modulated temporal IOIs. Time courses, GFPs, and scalp topographies of ‘repetition’- modulated and signed F values of AEPs (*top*), SEPs (*middle*), and NEPs (*bottom*). Time courses of signed F values from all electrodes are plotted in *different colors* and superimposed. Temporal IOIs, capturing MMN responses, are enclosed in *blue rectangles*. For AEPs, a MMN IOI was observed at 92–193 ms, showing a clear negativity at bilateral fronto-central region (maximal around FC1, FC2, FC3, and FC4). For SEPs, two MMN IOIs were observed at 64–160 ms and at 161–245 ms, showing a negativity at bilateral temporal regions (maximal around FC6, C6 and C6, CP6, respectively). For NEPs, a MMN IOI was observed at 155–273 ms, showing a clear negativity at bilateral temporal regions (maximal around FC6 and C6) (color figure online)



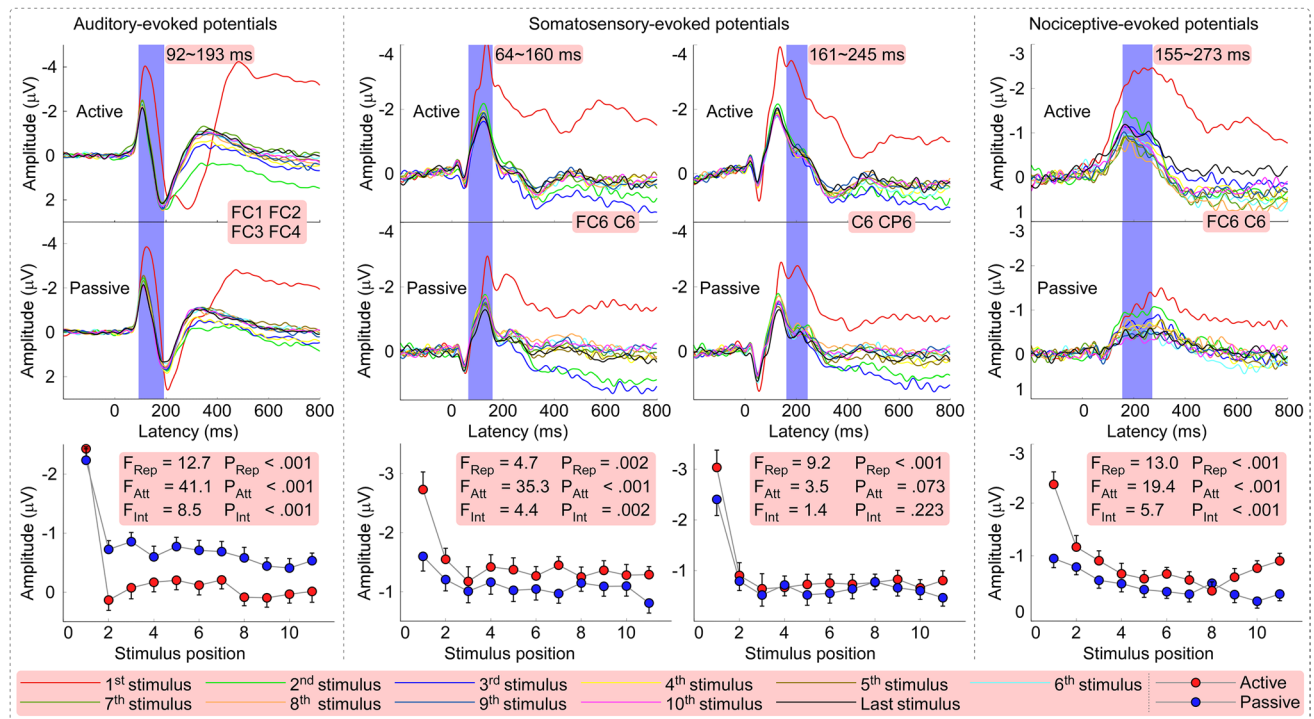


Fig. 3 Modulations by stimulus repetition within MMN IOIs in Active and Passive conditions. Time courses of AEPs (*left* measured at FC1, FC2, FC3, and FC4), SEPs (*middle* measured at FC6, C6 and C6, CP6, respectively), and NEPs (*right* measured at FC6, C6) to repeated stimuli (first, second, ..., tenth, and last). Signals are displayed for Active (*top* upper plots) and Passive (*top* lower plots) conditions, respectively. AEPs, SEPs, and NEPs from different positions in the train are plotted

ted in *different colors* and superimposed. MMN-related time intervals, defined by the topographical segmentation analysis, are highlighted in *violet*. Mean ERP amplitudes within the defined temporal IOIs are showed with *blue* and *red* dots for Active and Passive conditions, respectively (*bottom*). *F* values and *P* values representing the main effect of ‘repetition’ (*F_{Rep}*), ‘attention’ (*F_{Att}*), as well as their interaction (*F_{Int}*), are reported in the *insets* (color figure online)

$P < .001$), ‘attention’ ($F_{(1,29)} = 41.14, P < .001$), and their interaction ($F_{(1,29)} = 8.52, P < .001$) (Fig. 3, bottom left). Post hoc Tukey’s HSD test revealed that in both Active and Passive conditions, amplitudes of AEPs within the MMN IOI to the first stimulus were significantly different from amplitudes to stimulus in any other train position ($P < .001$ for all comparisons). Amplitudes varied negligibly after the second train position in Active condition, and after the third train position in Passive condition (Appendix 2, ESM). Amplitudes of SEPs within the first MMN IOI were significantly modulated by ‘repetition’ ($F_{(1,29)} = 4.74, P = .002$), ‘attention’ ($F_{(1,29)} = 35.28, P < .001$), and their interaction ($F_{(1,29)} = 4.43, P = .002$) (Fig. 3, bottom middle). Amplitudes of SEPs within the second MMN IOI were significantly modulated by ‘repetition’ ($F_{(1,29)} = 9.22, P < .001$), but not significantly modulated by ‘attention’ ($F_{(1,29)} = 3.46, P = .073$) and their interaction ($F_{(1,29)} = 1.37, P = .223$) (Fig. 3, bottom middle). Post hoc Tukey’s HSD test revealed that in both Active and Passive conditions, amplitudes of SEPs within both the first and second MMN IOIs to the first stimulus were significantly different from amplitudes to stimulus in any other train position ($P < .001$ for all comparisons).

Amplitudes of SEPs within both the first and second MMN IOIs changed minimally after the first train position in both Active and Passive conditions (Appendix 3, ESM). Amplitudes of NEPs within the MMN IOI were significantly modulated by ‘repetition’ ($F_{(1,29)} = 13.03, P < .001$), ‘attention’ ($F_{(1,29)} = 19.37, P < .001$), and their interaction ($F_{(1,29)} = 5.67, P < .001$) (Fig. 3, bottom right). Post hoc Tukey’s HSD test revealed that NEP amplitudes within the MMN IOI to the first stimulus were significantly different from amplitudes elicited by stimuli delivered in any other train position in Active condition ($P < .001$ for all comparisons), and from amplitudes elicited by stimuli delivered after the third train position in Passive condition ($P < .01$ for all comparisons). Amplitudes changed minimally after the third and second train positions in Active and Passive conditions, respectively (Appendix 4, ESM).

Features of MMN responses

Figure 4 shows the scalp topographies and time courses of AEPs, SEPs, NEPs within the MMN IOIs to the deviant (first stimulus in each train), standard (mean of fourth to the last stimuli) and their difference (deviant–standard) in

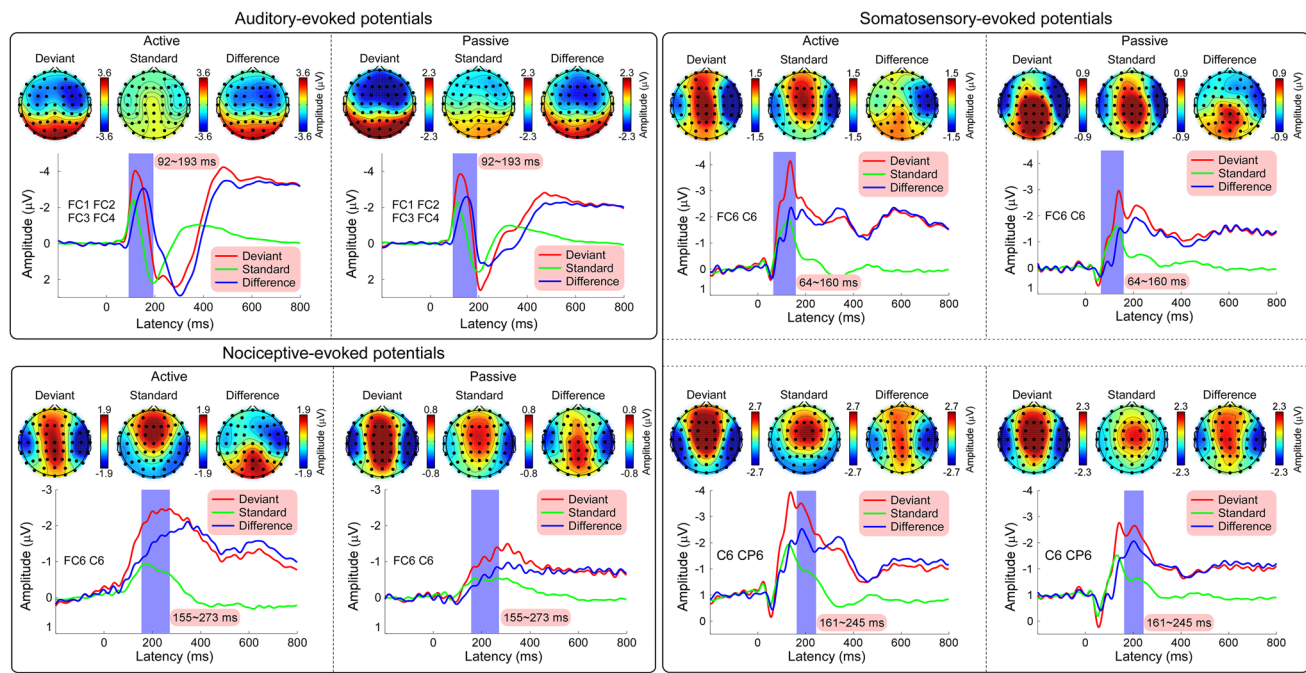


Fig. 4 Features of crossmodal MMN responses. Scalp representation of AEP (top left), SEP (right), and NEP (bottom left) amplitudes and their time courses elicited by the deviant (first stimulus in each train), standard (mean of fourth to last stimulus), and their difference

(deviant–standard), are displayed for Active and Passive conditions, respectively. Temporal IOIs (AEPs: 92–193 ms; SEPs: 64–160 ms and 161–245 ms; NEPs: 155–273 ms, defined by topographical segmentation analysis, are highlighted in *violet* (color figure online)

both Active and Passive conditions. The difference between deviant and standard of AEPs within the MMN IOI showed a negative maximum at fronto-central region in both Active and Passive conditions (FC1, FC2, FC3, and FC4) (Fig. 4; top left). The difference between deviant and standard of SEPs within the first MMN IOI displayed a negative maximum at contralateral fronto-temporal region in both Active and Passive conditions (FC6, C6) (Fig. 4, top right), while the difference between deviant and standard of SEPs within the second MMN IOI displayed a negative maximum at bilateral temporal regions in both Active and Passive conditions (larger at the contralateral side: C6, CP6) (Fig. 4, bottom right). The difference between deviant and standard of NEPs within the MMN IOI displayed a negative maximum at bilateral fronto-temporal electrodes in both Active and Passive conditions (larger at the contralateral side: FC6, C6) (Fig. 4, bottom left).

Figure 5 shows time courses of AEPs, SEPs, and NEPs elicited by deviant (first stimulus in each train) and standard (mean of fourth to the last stimuli) for each preceding sensory modality and attentional condition. Two-way repeated measures ANOVA revealed that amplitudes of AEPs to deviant stimuli were not significantly modulated by ‘preceding modality’ ($F_{(1,29)} = 2.69, P = .112$), ‘attention’ ($F_{(1,29)} = 1.50, P = .230$), and their interaction ($F_{(1,29)} = 2.24, P = .131$) (Fig. 5, top left). Amplitudes of SEPs to deviant stimuli were significantly modulated

by ‘preceding modality’ ($F_{(1,29)} = 19.41, P < .001$ within the first MMN IOI; $F_{(1,29)} = 22.12, P < .001$ within the second MMN IOI), ‘attention’ ($F_{(1,29)} = 29.16, P < .001$ within the first MMN IOI; $F_{(1,29)} = 4.87, P = .035$ within the second MMN IOI), but not by their interaction ($F_{(1,29)} = .46, P = .506$ within the first MMN IOI; $F_{(1,29)} = 1.72, P = .200$ within the second MMN IOI) (Fig. 5, top middle). Amplitudes of NEPs to deviant stimuli were significantly modulated by ‘preceding modality’ ($F_{(1,29)} = 7.49, P = .011$), ‘attention’ ($F_{(1,29)} = 20.07, P < .001$), and their interaction ($F_{(1,29)} = 5.13, P = .031$) (Fig. 5, top right). Post hoc Tukey’s HSD test revealed that when preceded by auditory trains, amplitudes of NEPs to deviant stimuli were significantly different from those preceded by non-nociceptive somatosensory trains in Active condition ($P = .003$), but not in Passive condition ($P = .636$). Amplitudes of AEPs, SEPs, and NEPs to standard stimuli were not significantly modulated by ‘preceding modality’ (AEPs: $F_{(1,29)} = .27, P = .607$; SEPs: $F_{(1,29)} = 3.78, P = .062$ and $F_{(1,29)} = 1.75, P = .196$; NEPs: $F_{(1,29)} = .92, P = .344$) and their interaction (AEPs: $F_{(1,29)} = .16, P = .695$; SEPs: $F_{(1,29)} = 1.54, P = .224$ and $F_{(1,29)} = .52, P = .477$; NEPs: $F_{(1,29)} = 1.95, P = .173$), but partly significantly modulated by ‘attention’ (AEPs: $F_{(1,29)} = 30.20, P < .001$; SEPs: $F_{(1,29)} = 20.20, P < .001$ and $F_{(1,29)} = 2.91, P = .099$; NEPs: $F_{(1,29)} = 7.45, P = .011$) (Fig. 5, bottom panels).

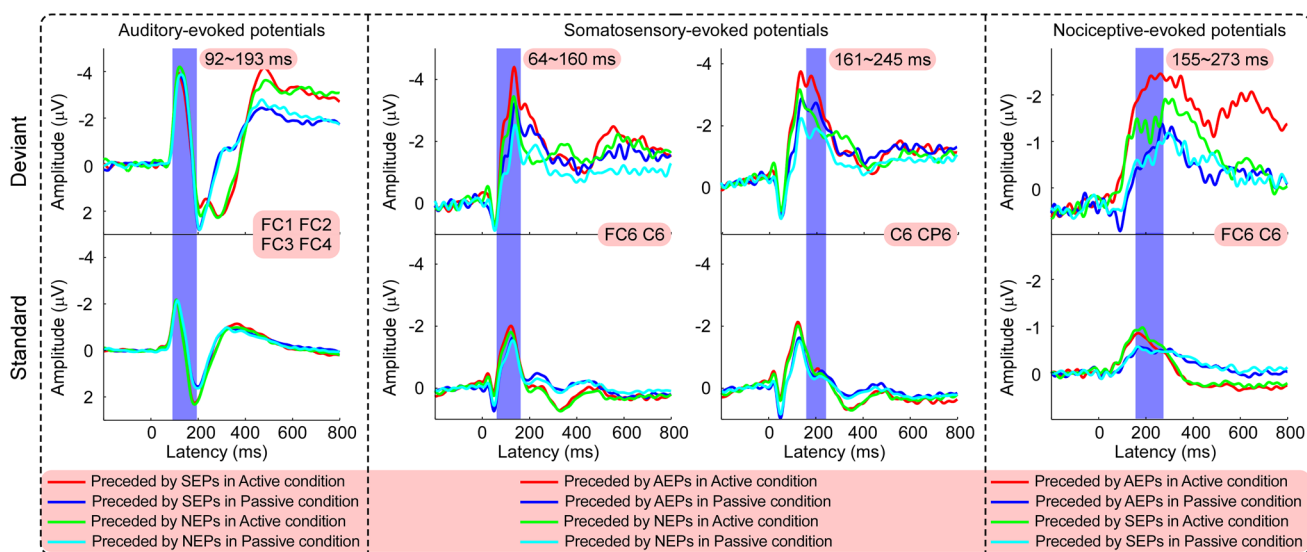


Fig. 5 Time courses of AEPs, SEPs, and NEPs to deviant and standard stimuli for each preceding sensory modality and attentional condition. Time courses of AEPs (*left* measured at FC1, FC2, FC3, and FC4), SEPs (*middle* measured at FC6, C6 and C6, CP6, respectively), and NEPs (*right* measured at FC6, C6) to deviant (*top*) and standard (*bottom*) stimuli. ERPs preceded by different sensory modalities, in both attentional conditions (Active and Passive), are plotted in *differ-*

ent colors and superimposed. Temporal IOIs, defined by topographical segmentation analysis, are highlighted in *violet*. Note that deviant-triggered SEPs and NEPs had lower amplitude when, respectively, preceded by nociceptive and non-nociceptive somatosensory trains than when preceded by an auditory train, especially when subjects actively attended to the stimuli (color figure online)

As summarized in Appendix 5 (A5, ESM), significant correlations were only observed between different amplitudes in the two attentional conditions for the same sensory modality (AEP MMN: $R = .76$, $P < .001$; SEP MMN within the first IOI: $R = .65$, $P < .001$; SEP MMN within the second IOI: $R = .76$, $P < .001$), except NEP MMN ($R = .43$, $P = .017$, did not survive after Bonferroni correction).

Discussion

In the present study, we used a crossmodal roving paradigm and applied a topographical segmentation analysis to directly compare mismatch responses across different sensory modalities (Fig. 1). We obtained three main findings. First, we identified a standard sensory event within each modality following at least two repetitions (i.e., after the third position in a train), regardless of the preceding sensory modality and attentional condition (Fig. 3). Second, we found that the somatosensory and nociceptive deviant activity was influenced by the modality of the preceding standard (Fig. 5). Third, we show that amplitudes of MMN covary significantly between Active and Passive conditions within the same sensory modality, but not between different sensory modalities (with the exception of the nociceptive MMN, which showed a lower signal-to-noise ratio than MMN in other sensory modalities).

Analytical approach to the extraction of MMN

To tackle the multiple comparisons problem and to control for the family-wise error rate, the cluster-based test was proposed for the statistical analysis of hemodynamic (Bullmore et al. 1999) and electrophysiological data (Maris and Oostenveld 2007). When applied to electrophysiological data, the clustering is achieved based on the temporal adjacency of statistical significance if data from single electrode are tested or based on the spatial and temporal adjacency of statistical significance if data from multi-electrodes are tested (Maris and Oostenveld 2007). This approach is suited to solve the multiple comparison problem and has been successfully applied in several studies (Lehmann et al. 2007; Kiiski et al. 2012; Hu et al. 2013; Stelzer et al. 2013). Despite the sensitivity of this approach, we found that when significant differences were large and persistent in time, the cluster-based approach resulted in a long-lasting temporal cluster. However, scalp regions that showed the large significance varied greatly within the extracted long-lasting temporal cluster (Appendix 1, ESM). In this case, the definition of the temporal IOI (cluster) cannot be optimally achieved using only the cluster-based approach. Therefore, we implemented a statistical approach that did not only detect the temporal adjacency of significances, but also incorporated the scalp distribution of these significances (signed F values), as to improve the definition of the temporal IOI. The use of the spatial information

was achieved by the topographical segmentation analysis, which is conceptually identical to the method of functional microstates (Lehmann et al. 1987).

The reliability of the application of the topographical segmentation analysis to extract MMN-related activity is supported by the fact that the MMN responses extracted in this study captured features (e.g., observed latency range and scalp topography) overly similar to classical MMN responses reported in previous studies. First, the obtained AEP MMN (92–193 ms) was showed to be maximal at fronto-central electrodes (Fig. 2, top), which was in line with most previous reports that described an auditory MMN between 100 and 250 ms and at fronto-temporal or fronto-central regions (Sams et al. 1985; Näätänen et al. 2011). Second, the extracted SEP MMN (64–160 and 161–245 ms) and NEP MMN (155–273 ms) were distributed at bilateral temporal regions with a maximum at the contralateral hemisphere (Fig. 2, middle and bottom), similarly to what has been previously observed for the somatosensory (Akatsuwa et al. 2007; Chen et al. 2008) and nociceptive MMN (Hu et al. 2013).

The establishment of deviant and standard ERPs in the roving paradigm

Traditionally, the MMN is conceived as the result of a comparison between ERPs evoked by deviant versus standard events. Therefore, the amplitude and topography of ERPs elicited by standard stimuli can determine the shape and amplitude of mismatch-related ERPs elicited by deviant stimuli (Cowan et al. 1993; Javitt et al. 1997; Bendixen et al. 2007). The correct functional identification of responses reflecting a standard event crucially affects the estimation of deviance-related responses. Surprisingly, the issue of *whether* and *when* a stimulus event can be considered as a standard has been overlooked so far (Sussman 2007). An important attempt has been provided by Haenschel et al. (2005), who investigated the role of stimulus repetition on ERPs to deviant and standard events. They revealed that the increase of stimulus repetition in a roving paradigm increased the MMN amplitude regardless of whether the subject was passively listening to or actively discriminating changes in tone frequency.

In the present study, we aimed to investigate whether standard formation could be influenced by (1) the number of repetitions in a train of stimuli with identical sensory properties and (2) the sensory modality of the preceding train of stimuli. Generally, by comparing amplitudes evoked by stimuli with different position in a train, we found no difference between amplitudes after the third train position across sensory modalities and attentional conditions (Fig. 3). This finding implied that identical sensory stimuli after the third position in a train could be considered

as robust standards in the roving paradigm. Importantly, the standard-related amplitude was not influenced by the amplitude of the standard in the preceding train and belonging to a different modality (Fig. 5), which suggests that the standard formation depends on the number of repetitions regardless of the preceding sensory modality.

In contrast, crossmodal deviant responses were significantly affected by the sensory modality of the preceding train (Fig. 5). For instance, SEPs evoked by the first stimulus of a somatosensory train were significantly larger following an auditory train than following a nociceptive train. Similarly, NEPs evoked by deviants were significantly larger following an auditory train than following a non-nociceptive somatosensory train. This observation indicates that the representation of a deviant is largely influenced by the preceding sensory modality of the standard.

Is MMN modality dependent or independent?

As different scalp topographies must be generated by different configuration of neural activations in the brain (Michel et al. 2004), neural sources of activities elicited by stimuli belonging to different sensory modalities should display clearly different topographical patterns. That the scalp topography of auditory MMN (maximal at fronto-central region, Fig. 4) was different from that of non-nociceptive somatosensory MMN and of nociceptive MMN (maximal at bilateral temporal regions, Fig. 4) is in agreement with several previous studies (Näätänen et al. 1978; Opitz et al. 2005; Akatsuwa et al. 2007; Garrido et al. 2007; Yucel et al. 2007; Butler et al. 2011, 2012). This finding supports the notion that MMN reflects, at least partly, the neural activation in the primary and secondary sensory cortices in a given sensory modality (Opitz et al. 2005; Garrido et al. 2007). Accordingly, differences in MMN latencies across different modalities are mainly caused by the difference in fibers conduction velocity (e.g., the A β fiber consists of large myelinated axons with faster conduction velocity than the thinly myelinated A δ fiber, which contributes to the earlier latency of somatosensory MMN than nociceptive MMN) (Ploner et al. 1999, 2000).

More importantly, we found that significant correlations of MMN amplitude took place between the two attentional conditions (Active vs. Passive) only within each sensory modality, but not between different sensory modalities (A5), with the exception of the NEPs. In other words, involuntary or voluntary attentional orientation reflected by MMN responses varied similarly within, but not between sensory modality. This interpretation would be consistent with several findings from the previous literature that concur to draw a picture where latencies, topographies, and even estimated sources hint to a clear anatomo-functional separation between the auditory and the somatosensory

modalities (Sams et al. 1985; Akatsuka et al. 2007; Garrido et al. 2009; Lozano-Soldevilla et al. 2012; Hu et al. 2013).

Yet, the notion that non-nociceptive somatosensory and nociceptive MMN would rely on separate sub-modality mechanisms is currently untenable. In agreement with our previous findings (Hu et al. 2013), scalp topographies of non-nociceptive somatosensory and nociceptive MMN were similarly maximal at bilateral temporal regions (Fig. 4). Although somatosensory and nociceptive cortical responses to deviant events may share similar generators, they may be independently represented and functionally segregated within the cortex (Ploner et al. 2000). This hypothesis is in agreement with the anatomo-physiological segregation of tactile/proprioceptive versus nociceptive representation in the periphery of the central nervous system (Ploner et al. 2000) as well as with other findings revealing partially overlapping cortical structures and dissimilar functional organization of somatosensory and nociceptive representations (Paxinos and Mai 2004; Ploner et al. 2004). In this vein, we found that the amplitudes of non-nociceptive somatosensory MMN and nociceptive MMN were not significant correlated, even within the same attentional condition (A5). This finding suggests that somatosensory and nociceptive MMN may be functionally dissociated although being generated from similar neural structures.

Theoretical scenario and conclusion

We found that the formation of a standard memory trace can be considered stable from the third stimulus position in a train, regardless of sensory modality and attentional condition. The gradual fading of amplitude differences across train positions confirms that standard formation does not obey the all-or-none law and rather rely on a progressive strengthening of the sensory memory trace (Baldeweg et al. 2004; Haenschel et al. 2005), as suggested by the model adjustment hypothesis (Winkler et al. 1996; Näätänen and Winkler 1999). In the context of the model adjustment hypothesis, the MMN is regarded as a marker for error detection, which is caused by a deviation from a learned regularity. It is noteworthy that in the context of the roving paradigm, there is no physical difference between the standard and the deviant, but the different position in the train. Therefore, the crossmodal roving paradigm maximized the contrast between the memory trace formed before the standard (i.e., third stimulus position) and the trace formed before the deviant (i.e., first stimulus position). Consequently, the previous modality had no influence on the standard formation while affecting that of the deviant (Fig. 5).

Our design cannot explain whether the effect of mismatch associated with the deviant was due to the change of stimulus modality or more generally to the temporal

unpredictability of the first stimulus in a train. However, Valentini et al. (2011), using equiprobable presentation of deviant events, showed that the reduction of ERPs amplitude due to stimulus repetition is largely affected by a change in a physical feature of the stimulation (e.g., modality) while being less sensitive to the fact that the incoming sensory stimulation is predictable/expected. Thus, we argue that the interpretation of our findings based solely on a temporal expectation account is unlikely and that the responses obtained using the crossmodal design largely reflect those obtained in unimodal/bimodal studies (auditory MMN: Sams et al. 1985; Näätänen et al. 2011; somatosensory MMN: Akatsuka et al. 2007; Chen et al. 2008; nociceptive MMN: Hu et al. 2013).

Importantly, the whole findings obtained in the deviance detection literature may also be interpreted according to the sensory adaptation hypothesis, by virtue of which the mismatch responses would result from a much simpler mechanism of local neuronal adaptation/refractoriness at the level of the sensory cortices. The scalp topographies elicited by deviant stimuli in AEPs (fronto-central), SEPs (temporo-parietal), and NEPs (fronto-temporal) would be compatible with the underlying activation of primary and secondary sensory cortices in the three sensory modalities (Fig. 4), as also suggested by other reports (Näätänen et al. 1978; Opitz et al. 2005; Akatsuka et al. 2007; Garrido et al. 2007; Yucel et al. 2007; Butler et al. 2011, 2012). Furthermore, the finding that MMN amplitudes varied between the two attentional conditions (Active vs. Passive) only within each sensory modality but not between different sensory modalities (A5) complements this notion. Indeed, findings obtained with MEG (Jääskeläinen et al. 2004; May and Tiitinen 2004) have been interpreted according to the notion that the auditory MMN is due to a delayed and amplitude-modulated N1 and shares its neural generators (May and Tiitinen 2010). According to May and Tiitinen (2010), there is virtually no means to separate the neural activation overlap determined by a standard and a deviant stimulus because these two stimuli might activate divergent populations but still elicit a similar N1 response, eventually suggesting that even the most subtle difference between deviants and standards will ensue in a N1-contaminated MMN.

In conclusion, notwithstanding the lack of consensus on whether the recording of a N1-uncontaminated MMN is methodologically feasible, our findings provide evidence that, while different modalities share a similar process of standard trace formation, the process of deviance detection is largely modality dependent.

Acknowledgments LH and CZ were supported by the National Natural Science Foundation of China (31200856, 31471082), Natural Science Foundation Project of CQ CSTC, and Fundamental Research Funds for the Central Universities (SWU1409105). CZ was supported by the program of China Scholarship Council (201406990026).

Conflict of interest The authors declare no competing financial interests.

References

- Akatsuka K, Wasaka T, Nakata H, Kida T, Hoshiyama M, Tamura Y, Kakigi R (2007) Objective examination for two-point stimulation using a somatosensory oddball paradigm: an MEG study. *Clin Neurophysiol* 118:403–411. doi:[10.1016/j.clinph.2006.09.030](https://doi.org/10.1016/j.clinph.2006.09.030)
- Baldeweg T, Klugman A, Gruzelier J, Hirsch SR (2004) Mismatch negativity potentials and cognitive impairment in schizophrenia. *Schizophr Res* 69:203–217
- Bendixen A, Roeber U, Schröger E (2007) Regularity extraction and application in dynamic auditory stimulus sequences. *J Cogn Neurosci* 19:1664–1677. doi:[10.1162/jocn.2007.19.10.1664](https://doi.org/10.1162/jocn.2007.19.10.1664)
- Bullmore ET, Suckling J, Overmeyer S, Rabe-Hesketh S, Taylor E, Brammer MJ (1999) Global, voxel, and cluster tests, by theory and permutation, for a difference between two groups of structural MR images of the brain. *IEEE Trans Med Imaging* 18:32–42
- Butler JS, Molholm S, Fiebelkorn IC, Mercier MR, Schwartz TH, Foxe JJ (2011) Common or redundant neural circuits for duration processing across audition and touch. *J Neurosci* 31:3400–3406. doi:[10.1523/JNEUROSCI.3296-10.2011](https://doi.org/10.1523/JNEUROSCI.3296-10.2011)
- Butler JS, Foxe JJ, Fiebelkorn IC, Mercier MR, Molholm S (2012) Multisensory representation of frequency across audition and touch: high density electrical mapping reveals early sensory–perceptual coupling. *J Neurosci* 32:15338–15344. doi:[10.1523/JNEUROSCI.1796-12.2012](https://doi.org/10.1523/JNEUROSCI.1796-12.2012)
- Cacace AT, McFarland DJ (2003) Quantifying signal-to-noise ratio of mismatch negativity in humans. *Neurosci Lett* 341:251–255
- Chen TL, Babiloni C, Ferretti A et al (2008) Human secondary somatosensory cortex is involved in the processing of somatosensory rare stimuli: an fMRI study. *Neuroimage* 40:1765–1771. doi:[10.1016/j.neuroimage.2008.01.020](https://doi.org/10.1016/j.neuroimage.2008.01.020)
- Cowan N, Winkler I, Teder W, Näätänen R (1993) Memory prerequisites of mismatch negativity in the auditory event-related potential (ERP). *J Exp Psychol Learn Mem Cogn* 19:909–921
- Crucu G, Aminoff MJ, Curio G et al (2008) Recommendations for the clinical use of somatosensory-evoked potentials. *Clin Neurophysiol* 119:1705–1719. doi:[10.1016/j.clinph.2008.03.016](https://doi.org/10.1016/j.clinph.2008.03.016)
- Delorme A, Makeig S (2004) EEGLAB: an open source toolbox for analysis of single-trial EEG dynamics including independent component analysis. *J Neurosci Methods* 134:9–21. doi:[10.1016/j.jneumeth.2003.10.009](https://doi.org/10.1016/j.jneumeth.2003.10.009)
- Doeller CF, Opitz B, Mecklinger A, Krick C, Reith W, Schröger E (2003) Prefrontal cortex involvement in preattentive auditory deviance detection: neuroimaging and electrophysiological evidence. *Neuroimage* 20:1270–1282. doi:[10.1016/S1053-8119\(03\)00389-6](https://doi.org/10.1016/S1053-8119(03)00389-6)
- Garcia-Larrea L, Lukaszewicz AC, Mauguire F (1995) Somatosensory responses during selective spatial attention: the N120-to-N140 transition. *Psychophysiology* 32:526–537
- Garrido MI, Kilner JM, Kiebel SJ, Stephan KE, Friston KJ (2007) Dynamic causal modelling of evoked potentials: a reproducibility study. *Neuroimage* 36:571–580. doi:[10.1016/j.neuroimage.2007.03.014](https://doi.org/10.1016/j.neuroimage.2007.03.014)
- Garrido MI, Friston KJ, Kiebel SJ, Stephan KE, Baldeweg T, Kilner JM (2008) The functional anatomy of the MMN: a DCM study of the roving paradigm. *Neuroimage* 42:936–944. doi:[10.1016/j.neuroimage.2008.05.018](https://doi.org/10.1016/j.neuroimage.2008.05.018)
- Garrido MI, Kilner JM, Kiebel SJ, Friston KJ (2009) Dynamic causal modeling of the response to frequency deviants. *J Neurophysiol* 101:2620–2631. doi:[10.1152/jn.90291.2008](https://doi.org/10.1152/jn.90291.2008)
- Haenschel C, Vernon DJ, Dwivedi P, Gruzelier JH, Baldeweg T (2005) Event-related brain potential correlates of human auditory sensory memory-trace formation. *J Neurosci* 25:10494–10501. doi:[10.1523/JNEUROSCI.1227-05.2005](https://doi.org/10.1523/JNEUROSCI.1227-05.2005)
- Hu L, Zhang ZG, Hung YS, Luk KD, Iannetti GD, Hu Y (2011) Single-trial detection of somatosensory evoked potentials by probabilistic independent component analysis and wavelet filtering. *Clin Neurophysiol* 122:1429–1439. doi:[10.1016/j.clinph.2010.12.052](https://doi.org/10.1016/j.clinph.2010.12.052)
- Hu L, Zhao C, Li H, Valentini E (2013) Mismatch responses evoked by nociceptive stimuli. *Psychophysiology* 50:158–173. doi:[10.1111/psyp.12000](https://doi.org/10.1111/psyp.12000)
- Inui K, Tran TD, Hoshiyama M, Kakigi R (2002) Preferential stimulation of Adelta fibers by intra-epidermal needle electrode in humans. *Pain* 96:247–252
- Inui K, Tsuji T, Kakigi R (2006) Temporal analysis of cortical mechanisms for pain relief by tactile stimuli in humans. *Cereb Cortex* 16:355–365. doi:[10.1093/cercor/bhi114](https://doi.org/10.1093/cercor/bhi114)
- Jääskeläinen IP, Ahveninen J, Bonmassar G et al (2004) Human posterior auditory cortex gates novel sounds to consciousness. *Proc Natl Acad Sci USA* 101:6809–6814
- Javitt DC, Strous RD, Grochowski S, Ritter W, Cowan N (1997) Impaired precision, but normal retention, of auditory sensory (“echoic”) memory information in schizophrenia. *J Abnorm Psychol* 106:315–324
- Kekoni J, Hamalainen H, Saarinen M, Grohn J, Reinikainen K, Lehtokoski A, Näätänen R (1997) Rate effect and mismatch responses in the somatosensory system: ERP-recordings in humans. *Biol Psychol* 46:125–142
- Kiiski H, Reilly RB, Lonergan R et al (2012) Only low frequency event-related EEG activity is compromised in multiple sclerosis: insights from an independent component clustering analysis. *PLoS One* 7:e45536. doi:[10.1371/journal.pone.0045536](https://doi.org/10.1371/journal.pone.0045536)
- Lehmann D, Skrandies W (1980) Reference-free identification of components of checkerboard-evoked multichannel potential fields. *Electroencephalogr Clin Neurophysiol* 48:609–621
- Lehmann D, Ozaki H, Pal I (1987) EEG alpha map series: brain micro-states by space-oriented adaptive segmentation. *Electroencephalogr Clin Neurophysiol* 67:271–288
- Lehmann C, Koenig T, Jelic V et al (2007) Application and comparison of classification algorithms for recognition of Alzheimer’s disease in electrical brain activity (EEG). *J Neurosci Methods* 161:342–350. doi:[10.1016/j.jneumeth.2006.10.023](https://doi.org/10.1016/j.jneumeth.2006.10.023)
- Liang M, Mouraux A, Chan V, Blakemore C, Iannetti GD (2010) Functional characterisation of sensory ERPs using probabilistic ICA: effect of stimulus modality and stimulus location. *Clin Neurophysiol* 121:577–587. doi:[10.1016/j.clinph.2009.12.012](https://doi.org/10.1016/j.clinph.2009.12.012)
- Lozano-Soldevilla D, Marco-Pallares J, Fuentemilla L, Grau C (2012) Common N1 and mismatch negativity neural evoked components are revealed by independent component model-based clustering analysis. *Psychophysiology* 49:1454–1463. doi:[10.1111/j.1469-8986.2012.01458.x](https://doi.org/10.1111/j.1469-8986.2012.01458.x)
- MacDonald DB, Stigsby B, Al Zayed Z (2004) A comparison between derivation optimization and Cz’-FPz for posterior tibial P37 somatosensory evoked potential intraoperative monitoring. *Clin Neurophysiol* 115:1925–1930. doi:[10.1016/j.clinph.2004.03.008](https://doi.org/10.1016/j.clinph.2004.03.008)
- Maris E, Oostenveld R (2007) Nonparametric statistical testing of EEG- and MEG-data. *J Neurosci Methods* 164:177–190. doi:[10.1016/j.jneumeth.2007.03.024](https://doi.org/10.1016/j.jneumeth.2007.03.024)
- May PJ, Tiitinen H (2004) Auditory scene analysis and sensory memory: the role of the auditory N100m. *Neurol Clin Neurophysiol* 2004:19
- May PJ, Tiitinen H (2010) Mismatch negativity (MMN), the deviance-elicited auditory deflection, explained. *Psychophysiology* 47:66–122. doi:[10.1111/j.1469-8986.2009.00856.x](https://doi.org/10.1111/j.1469-8986.2009.00856.x)
- Michel CM, Thut G, Morand S et al (2001) Electric source imaging of human brain functions. *Brain Res Rev* 36:108–118
- Michel CM, Murray MM, Lantz G, Gonzalez S, Spinelli L, Grave de Peralta R (2004) EEG source imaging. *Clin Neurophysiol* 115:2195–2222. doi:[10.1016/j.clinph.2004.06.001](https://doi.org/10.1016/j.clinph.2004.06.001)

- Miura T, Sonoo M, Shimizu T (2003) Establishment of standard values for the latency, interval and amplitude parameters of tibial nerve somatosensory evoked potentials (SEPs). *Clin Neurophysiol* 114:1367–1378
- Mouraux A, Iannetti GD, Plaghki L (2010) Low intensity intra-epidermal electrical stimulation can activate Adelta-nociceptors selectively. *Pain* 150:199–207. doi:[10.1016/j.pain.2010.04.026](https://doi.org/10.1016/j.pain.2010.04.026)
- Murray MM, Brunet D, Michel CM (2008) Topographic ERP analyses: a step-by-step tutorial review. *Brain Topogr* 20:249–264. doi:[10.1007/s10548-008-0054-5](https://doi.org/10.1007/s10548-008-0054-5)
- Näätänen R, Winkler I (1999) The concept of auditory stimulus representation in cognitive neuroscience. *Psychol Bull* 125:826–859
- Näätänen R, Gaillard AW, Mantysalo S (1978) Early selective-attention effect on evoked potential reinterpreted. *Acta Psychol* 42:313–329
- Näätänen R, Teder W, Alho K, Lavikainen J (1992) Auditory attention and selective input modulation: a topographical ERP study. *NeuroReport* 3:493–496
- Näätänen R, Paavilainen P, Rinne T, Alho K (2007) The mismatch negativity (MMN) in basic research of central auditory processing: a review. *Clin Neurophysiol* 118:2544–2590. doi:[10.1016/j.clinph.2007.04.026](https://doi.org/10.1016/j.clinph.2007.04.026)
- Näätänen R, Kujala T, Kreegipuu K, Carlson S, Escera C, Baldeweg T, Ponton C (2011) The mismatch negativity: an index of cognitive decline in neuropsychiatric and neurological diseases and in ageing. *Brain* 134:3435–3453. doi:[10.1093/brain/awr064](https://doi.org/10.1093/brain/awr064)
- Opitz B, Schröger E, Von Cramon D (2005) Sensory and cognitive mechanisms for preattentive change detection in auditory cortex. *Eur J Neurosci* 21:531–535
- Pakarinen S, Huotilainen M, Näätänen R (2010) The mismatch negativity (MMN) with no standard stimulus. *Clin Neurophysiol* 121:1043–1050
- Pascual-Marqui RD, Michel CM, Lehmann D (1995) Segmentation of brain electrical activity into microstates: model estimation and validation. *IEEE Trans Biomed Eng* 42:658–665. doi:[10.1109/10.391164](https://doi.org/10.1109/10.391164)
- Paxinos G, Mai JK (2004) The human nervous system. Academic Press, San Diego
- Ploner M, Schmitz F, Freund HJ, Schnitzler A (1999) Parallel activation of primary and secondary somatosensory cortices in human pain processing. *J Neurophysiol* 81:3100–3104
- Ploner M, Schmitz F, Freund HJ, Schnitzler A (2000) Differential organization of touch and pain in human primary somatosensory cortex. *J Neurophysiol* 83:1770–1776
- Ploner M, Pollok B, Schnitzler A (2004) Pain facilitates tactile processing in human somatosensory cortices. *J Neurophysiol* 92:1825–1829. doi:[10.1152/jn.00260.2004](https://doi.org/10.1152/jn.00260.2004)
- Sams M, Hamalainen M, Antervo A, Kaukoranta E, Reinikainen K, Hari R (1985) Cerebral neuromagnetic responses evoked by short auditory stimuli. *Electroencephalogr Clin Neurophysiol* 61:254–266
- Stelzer J, Chen Y, Turner R (2013) Statistical inference and multiple testing correction in classification-based multi-voxel pattern analysis (MVPA): random permutations and cluster size control. *Neuroimage* 65:69–82. doi:[10.1016/j.neuroimage.2012.09.063](https://doi.org/10.1016/j.neuroimage.2012.09.063)
- Sussman ES (2007) A new view on the MMN and attention debate. *J Psychophysiol* 21:164–175
- Torta DM, Liang M, Valentini E, Mouraux A, Iannetti GD (2012) Dishabituation of laser-evoked EEG responses: dissecting the effect of certain and uncertain changes in stimulus spatial location. *Exp Brain Res* 218:361–372. doi:[10.1007/s00221-012-3019-6](https://doi.org/10.1007/s00221-012-3019-6)
- Valentini E, Torta DM, Mouraux A, Iannetti GD (2011) Dishabituation of laser-evoked EEG responses: dissecting the effect of certain and uncertain changes in stimulus modality. *J Cogn Neurosci* 23:2822–2837. doi:[10.1162/jocn.2011.21609](https://doi.org/10.1162/jocn.2011.21609)
- Winkler I, Karmos G, Näätänen R (1996) Adaptive modeling of the unattended acoustic environment reflected in the mismatch negativity event-related potential. *Brain Res* 742:239–252
- Yucel G, McCarthy G, Belger A (2007) fMRI reveals that involuntary visual deviance processing is resource limited. *Neuroimage* 34:1245–1252. doi:[10.1016/j.neuroimage.2006.08.050](https://doi.org/10.1016/j.neuroimage.2006.08.050)